2

CONF-8305127--5

UCRL-89981
PREPRINT

UCRL--89981

DE84 014637

WAVELENGTH SCALING OF LASER PLASMA COUPLING

W. L. Kruer

This paper was prepared for the proceedings for the Spring College on Radiation in Plasmas held in Trieste, Italy, May 24-June 17, 1983

November 3, 1983

Lawrence Livermore National Laboratory

Wavelength Scaling of Laser Plasma Coupling

W. L. Kruer

Lawrence Livermore National Laboratory

Abstract

The use of shorter wavelength laser light both enhances collisional absorption and reduces deleterious collective plasma effects. Coupling processes which can be important in reactor-size targets are briefly reviewed. Simple estimates are presented for the intensity-wavelength regime in which collisional absorption is high and collective effects are minimized.

*Work performed under the auspices of the U. S. Department of Energy by the Lawrence Livermore National Laboratory under contract number W-7405-ENG-48.

Laser plasma coupling can be influenced by a rich variety of collective plasma effects. Many of these collective effects either decrease the absorption or give absorption into a tail of very energetic electrons. These features of the coupling have placed a premium on the use of short wavelength laser light. As the wavelength (λ_0) of the light is decreased, the light penetrates to higher density plasma since the critical density (n_{cr}) increases as λ_0^{-2}. For a given absorbed intensity, the heated plasma, both denser and lower in temperature, is then much more collisional. The greater collisionality both enhances collisional absorption and reduces collective plasma effects.

The qualitative advantages of shorter wavelength light have long been recognized.[1] The thrust of the laser fusion program to shorter wavelength began in great ernest when deleterious collective effects emerged at unacceptable levels in implosion experiments with 1.06 μ light. Theoretical estimates[2,3] emphasized that the collective effects would be much reduced as the wavelength was decreased, and many experiments[4-6] throughout the world demonstrated the improved coupling.

Let us start our discussion of wavelength scaling by indicating the general region of parameter space of interest for laser fusion applications. A very important characteristic of a reactor target is the large size of the underdense plasma. The characteristic size, R, is typically of the order of 1/2 cm, which corresponds to many thousands of laser-light wavelengths for 1.06 μ light. The peak intensity of the light used to drive the target can vary considerably with the details of the design. Typically the peak intensity is in the range of 10^{14}-10^{16} W/cm^2.

Both the absorption efficiency and the heated velocity distribution are crucial features of the laser target coupling. It is optimum to directly heat as many electrons as is possible and, in particular, to avoid the generation of extremely energetic tails of hot electrons, which can preheat the inner fuel due to their long range. Preheat is a very important issue, since it can preclude achievement of the very large compression[1] needed for ignition and burn. In practice, less than 0.1% of the input energy can be allowed to end up as preheat in the fuel. Depending upon details of the target design, electrons with energy of order 50-100 keV can preheat the fuel. If an appreciable number of such electrons are generated, a thicker ablator is required, which increases the energy needed to drive the target.

WAVELENGTH SCALILNG OF INVERSE BREMSSTRAHLUNG ABSORPTION

The optimum absorption mechanism is also the simplest - inverse bremsstrahlung absorption. In the classical limit, inverse bremsstrahlung is just collisional heating. As electrons oscillate in the electric field of the laser light, they are randomly scattered by the ions. Coherent energy of oscillation is thereby converted into random thermal energy. The heating rate is then the oscillatory energy times the electron-ion collision frequency, ν_{ei}. By conservation of energy, this heating represents a damping of the light wave. Hence

$$\frac{\nu E_L^{\,2}}{8\pi} = \nu_{ei} \frac{nm\, v_{os}^2}{2} , \qquad (1)$$

where $v_{os} = eE_L/m\omega_0$, n is the plasma density, E_L and ω_0 are the electric field and frequency of the light wave, and ν is an effective collision frequency which describes the damping of the light wave. This damping rate is then[7]

$$\nu = \frac{n}{n_{cr}} \nu_{ei} \simeq (3 \times 10^{-6}) \ln \Lambda \frac{nZ}{\theta_{ev}{}^{3/2}} \frac{n}{n_{cr}} \quad , \qquad (2)$$

where Z is the ion charge state, θ_{ev} is the electron temperature (in eV), n_{cr} is the critical density, and Λ is the ratio of the maximum (b_{max}) and minimum (b_{min}) impact parameters. In particular, $b_{max} \simeq v_e/\omega_0$ and b_{min} is the greater of Ze^2/mv_e^2 or $\hbar/mv_e$, where $\hbar$ is Planck's constant and v_e is the electron thermal velocity. Note that ν has dependences which are characteristic of the properties of Coulomb collisions; i.e., ν increases with density and charge state and decreases as the plasma heats. The absorption length is the velocity of light divided by ν. It is apparent that this absorption can be very high in large regions of underdense plasma. It is also apparent that the slower electrons are preferentially heated, since the electron-ion collision frequency varies as v^{-3}, where v is the velocity of an electron. Hence inverse bremsstrahlung produces "soft" heated electron distributions.

Although the major dependences of the electron-ion collision frequency can be simply estimated using the Coulomb force law, a more detailed treatment is necessary to ensure the proper averaging over the velocity distribution of the electrons and to illustrate the heated distributions. Since in laser fusion applications the photon energy is much less than the electron temperature, the classical and quantum descriptions agree except for minor modifications. So we begin with the kinetic equation for a plasma with uniform density n, treating the electric field of the light wave in the dipole approximation; i.e. $E = E_0 \cos \omega_0 t$. Then

$$\frac{\partial f}{\partial t} - \frac{e}{m} \underset{\sim}{E} \cdot \frac{\partial f}{\partial \underset{\sim}{v}} = A \frac{\partial}{\partial \underset{\sim}{v}} \cdot \frac{v^2 \underset{\approx}{I} - \underset{\sim}{v}\underset{\sim}{v}}{v^3} \cdot \frac{\partial f}{\partial \underset{\sim}{v}} + C_{ee}(f) \quad , \tag{3}$$

where f is the distribution function of electrons and $A = 2\pi n Z e^4/m^2 \ln \Lambda$. The first term on the right-hand side describes electron-ion collisions, and $C_{ee}(f)$ denotes the operator describing electron-electron collisions.

For low intensity light [$(v_{os}/v_e)^2 << 1$, where v_{os} is again the oscillatory velocity of electrons in the light wave], the calculation is straight forward.[8] Expanding the distribution function as $f = f_0(v) + f_1(v) \cos\theta$, when θ is the angle between v and E, we obtain

$$\frac{\partial f_1}{\partial t} - \frac{eE}{m} \frac{\partial f_0}{\partial v} = - \frac{2A}{v^3} f_1 \quad . \tag{4}$$

Solving for f_1 and computing $\underset{\sim}{J}_1 = -e \int f_1 \underset{\sim}{v} d\underset{\sim}{v}$, we can then readily calculate the average rate of energy absorption by the plasma:

$$< \underset{\sim}{J}_1 \cdot \underset{\sim}{E} > = - \frac{4\pi}{3} A\, n\, m\, v_{os}^2 \int_0^\infty dv \frac{\partial f_0}{\partial v} g(v) \quad , \tag{5}$$

where $g(v) = [1 + (\frac{2A}{v^3 \omega})^2]^{-1}$. As long as $(\frac{2A}{\omega})^{1/3} << v_e$, $g(v) \simeq 1$ and

$$< \underset{\sim}{J}_1 \cdot \underset{\sim}{E} > \simeq \frac{4\pi}{3} A\, n m\, v_{os}^2\, f_0(0) \quad . \tag{6}$$

Noting that $< \underset{\sim}{J}_1 \cdot \underset{\sim}{E} > = \frac{\nu E^2}{8\pi}$ then gives

$$\nu \simeq \frac{\omega_{pe}^2}{\omega_o^2} \frac{8\pi}{3} A\, f_o(0) \quad , \tag{7}$$

where ω_{pe} is the electron plasma frequency.

The damping rate depends on the zero-order distribution function. The form of this distribution function in turn depends on whether electron-electron collisions (with frequency ν_{ee}) can equilibrate the distribution faster than electron-ion collisions cause it to heat. If $\nu_{ee} v_e^2 >> \nu_{ei} v_{os}^2$ (i.e., if $Z\, v_{os}^2/v_e^2 << 1$), the distribution function remains Maxwellian. We then obtain the result usually quoted in the literature and the one used in Eq. (2):

$$\nu \simeq \frac{\omega_{pe}^2}{\omega_o^2} \frac{1}{3(2\pi)^{3/2}} \frac{Z\, \omega_{pe}^4}{n\, v_e^3} \ln \Lambda \quad . \tag{8}$$

However, if $Z\, v_{os}^2/v_e^2 >> 1$, electron-electron collisions cannot equilibrate the distribution function sufficiently rapidly, and the form of the distribution function becomes determined by the collisional heating. In this limit, we return to the kinetic equation to obtain

$$\frac{\partial f_o}{\partial t} = \frac{eE}{m} \frac{1}{3v^2} \frac{\partial}{\partial v} (v^2 f_1) \quad . \tag{9}$$

Substituting for f_1, approximating $g(v) \simeq 1$, and looking for a self-similar solution, we find

$$f_o \sim \frac{1}{u^3} e^{-\frac{1}{5}\left(\frac{v}{u}\right)^5} \quad , \tag{10}$$

where $u = \left(\frac{5Av_{os}^2}{3} t\right)^{1/5}$. Hence the self-consistent distribution function is super-Gaussian in this limit. Since the distribution is rather flat-topped, there are fewer particles near $v \simeq 0$, and the collisional damping rate is reduced by a factor of $\simeq 2$.

Although quantitative calculations of the collisional absorption of course depend on the details of the density profile and the plasma temperature (i.e., heat transport), it is instructive to make some crude estimates which illustrate when this absorption can be efficient. The condition that the absorption be > 70% is that the density gradient length, R, of the underdense plasma near the critical density be greater than an absorption length; i.e., $\nu_{ei}R/c > 1$. We next relate the plasma temperature to the laser light intensity I via a free-streaming estimate which allows for moderate electron transport; i.e., $I \simeq .1\, n\theta_e v_e$. Combining these estimates gives a bound on the intensity in W/cm^2:

$$I < 5 \times 10^{14} \frac{Z\, R(cm)}{\lambda_\mu^4} , \qquad (11)$$

where Z is the ion charge, R the plasma scale length in cm, and λ_μ the laser light wave length in microns. For reactor targets, $R \sim 0.5$ cm. Hence $I < 2.5 \times 10^{14}\, Z/\lambda_\mu^4$, which is a readily accessible intensity for target design using lasers with $\lambda_\mu < 1$. The wavelength enters so strongly since $\nu_{ei} \sim n/\theta_e^{3/2}$. As the wavelength decreases, the light propagates through denser plasma which is also cooler.

Recent experiments [(4-6)] with .53 μ - .26 μ light are quite consistent with our simple estimates of inverse-bremsstrahlung absorption. For example, in LLNL experiments[(6)] in which gold targets were irradiated with .53 μ light, the measured absorption was greater than 70% for $I < 3 \times 10^{15}$ W/cm^2. If we estimate an ion charge state of 30 and a plasma size of $\sim$ 100 μ for these experiments, Eq. (11) gives $I < 2 \times 10^{15}$ W/cm^2. When Be (Z = 4) targets were irradiated, the absorption dropped below 70% for an intensity which was about a factor of ten lower, again as expected. These are very promising results, indicating that there is a significant classical regime available for target design using short wavelength lasers.

WAVELENGTH SCALING OF COLLECTIVE EFFECTS

The above rather idealized discussion indicates that collisional absorption can be sufficiently potent to give good absorption for short wavelength laser light. The key question then becomes: are collective plasma effects sufficiently suppressed? Since inverse bremsstrahlung is most effective near the critical density, collective effects at lower density can in principle still spoil the coupling.

We note that requiring collisional absorption of the light wave before it reaches a density $n << n_{cr}$ would strongly reduce the range of permissible intensities. For example, we use the condition that $\frac{\nu R}{c} > 2$, where $\nu = \nu_{ei} \frac{n}{n_{cr}}$ and R is now the local scale length at density n. Relating the plasma temperature to the intensity as before, we obtain

$$I < 2.5 \times 10^{14} \frac{Z\ R(cm)}{\lambda_\mu^4} \left(\frac{n}{n_{cr}}\right)^3 \quad . \tag{12}$$

Note that the permissible intensity is reduced from that given in Eq. (11) by the factor of about $\frac{1}{2} \left(\frac{n}{n_{cr}}\right)^3$. The estimated dependence on density is so strong, since $\nu = \frac{n}{n_{cr}} \nu_{ei}$, $\nu_{ei} \propto \frac{n\ Z}{\theta_e^{2/3}}$, and $\frac{1}{\theta_e^{3/2}} \propto n$.

This naturally brings us to a discussion of the other coupling mechanisms, which are related to collective plasma effects. It is well-known that, due to the long range of the Coulomb force, a plasma supports waves. These are collective modes of oscillation, which correspond to charge density fluctuations. In laser fusion applications, there are primarily two plasma waves of interest. The first is a high frequency electron plasma wave which occurs at the natural frequency with which electrons oscillate. The second is a low frequency ion acoustic wave, which is the analogue of a sound wave in an ordinary gas. The important point is that the laser light can excite these waves, which in turn can heat the plasma and/or scatter the light. In other words, collective effects can either increase or decrease the absorption.

Just as importantly, collective processes can change the character of the absorption. We've already pointed out that collisional absorption generates soft heated velocity distributions. In marked contrast, absorption via plasma waves typically leads to suprathermal electron generation. Consider an electrostatic wave with electric field $E \sin(kx - \omega t)$. Slow electrons just experience an oscillatory motion, which in the absence of collisions leads to no heating. However, fast electrons (i.e., those with $v \sim \omega/k >> v_e$) see a nearly constant field and can be efficiently accelerated. Hence, faster electrons are preferentially heated, leading to a heated velocity distribution characterized by energetic tails.

Resonance Absorption

Resonance absorption is the simplest example of absorption via plasma waves. The physics of this coupling is straight-forward. Consider a plasma with density $n(x)$ and a high frequency electric field, $E_L \sin \omega_0 t$, which oscillates electrons along the density gradient. This oscillation clearly generates a charge density fluctuation, δn, at frequency ω_0:

$$\delta n = n(x + x_{os}) - n(x) \simeq \underset{\sim}{x}_{os} \cdot \nabla n \quad ,$$

where $x_{os} = -eE_L/m\omega_0^2 \cos \omega_0 t$. Hence, whenever a component of the laser light electric field, E_L, oscillates electrons along a variation in density, a charge density fluctuation is directly driven. Near the critical density, this driven fluctuation is at just the frequency at which the plasma naturally responds, and so an electron plasma wave is resonantly excited. For high intensity light, the plasma wave grows in amplitude until it saturates by accelerating electrons, producing energetic tails. Note that resonance absorption takes place whenever $\underset{\sim}{E}_L \cdot \nabla n \neq 0$; i.e., for so-called p-polarized light.

Since resonance absorption operates on the zero-order density gradient due to plasma expansion, it is a fairly ubiquitous phenonmenon and has been the subject of many calculations.[10-11] Although resonance absorption is basically a linear process, nonlinear effects play a crucial role in the heating. Important features predicted quite some time ago were (1) nonlinear steepening of the density profile near the critical density due to the pressure of the locally generated plasma wave and the reflecting light wave, (2) polarization-dependent absorption, which is partially reduced by critical surface rippling, (3) an absorption efficiency of typically about 20-30% when averaged over the rippled surface and (4) heated electrons in a quasi-Maxwellian distribution with a temperature scaling as $(I\lambda_0^2)^{.4}$, where I is the intensity of the light and λ_0 is the wavelength. Resonance absorption is clearly less of an issue for short wavelength lasers both because inverse bremsstrahlung reduces the amount of light reaching the critical surface and because the resonantly- heated electron temperature decreases.

The calculations of resonance absorption have been supported by many different experiments[11] with high intensity laser light and small underdense plasmas. Of particular interest to the issue of wavelength scaling are recent experiments[4] at Ecole Polytechnique with 1 μ, 1/2 μ, and 1/4 μ laser light. High energy x-ray data from these experiments indicate that the resonantly-heated electron temperature scales as $(I\lambda_0^2)^{.46}$. Both the magnitude of the temperature and its scaling appear to be in quite reasonable agreement with calculations.

Plasma Instabilities

Collective effects can become considerably more complex for intense laser light in the large regions of underdense plasma characteristic of reactor targets. This complexity is primarily because plasma waves are also excited by instabilities.[12] As shown in Table I, most of these instabilities can be most simply described as the resonant decay of the laser light into two other waves. The frequency matching conditions then determine the region of plasma density for which the various instabilities occur. The ion-acoustic-decay instability corresponds to decay of the light wave into an ion acoustic wave plus an electron plasma wave and takes place near the critical density, n_{cr}. If the product waves are two electron plasma waves, we have the two-plasmon-decay ($2\ \omega_{pe}$) instability, which occurs near 1/4 n_{cr}. The Raman instability represents the decay of the light wave into a scattered light wave plus an electron plasma wave, a process which occurs for $n < 1/4\ n_{cr}$. The analogous scattering process in which the electron plasma wave is replaced by an ion acoustic wave is called the Brillouin instability. This instability operates throughout the underdense plasma. Finally there's the filamentation instability, a process which also occurs for $n < n_{cr}$. Any local increase in the laser light intensity pushes plasma aside, either directly via the enhanced light pressure or indirectly via enhanced heating and subsequent expansion. By refracting the light rays inward, this density depression further enhances the intensity. The net result can be the break-up of the incident light beam into intense filaments. Self-focusing of the entire light beam is a subset of this instability.

The Raman and 2 ω_{pe} Instabilities

Wherever one of the product waves is an electron plasma wave, very energetic electrons can be generated. The ion-acoustic-decay instability, which takes place near the critical density, tends to be limited by the steepening of the density profile which occurs there and by collisional absorption which reduces the intensity reaching the critical density. Of particular concern for hot electron generation are the two-plasmon-decay instability ($n \simeq 1/4\ n_{cr}$) and the Raman instability which produces its most energetic electrons near $1/4\ n_{cr}$. Computer simulations[13] of these instabilities in large regions of plasma with density near $1/4\ n_{cr}$ show more than 10% absorption into electrons with a characteristic temperature of order 100 keV.

The linear theory of these instabilities allows us to estimate their threshold intensities as a function of laser light wavelength. As a first approximation, the threshold intensity is generally set by the density gradient, which limits the region over which the resonant coupling can be satisified:

$$I_T \sim \frac{5 \times 10^{15} \theta_{keV}}{L_\mu \lambda_\mu} \qquad 2\,\omega_{pe} \text{ instability} \tag{13}$$

$$I_T \sim 10^{17} \frac{1}{L_\mu^{4/3} \lambda_\mu^{2/3}} \qquad \text{Raman instability near } \frac{1}{4} n_{cr} \text{ or Raman side scatter}$$

where I_T is the intensity in W/cm^2, θ_{keV} is the electron temperature in keV, and L_μ (λ_μ) is the local density gradient length (laser light wavelength) in microns. Note that, for $L_\mu \sim 2 \times 10^3$, the threshold intensities due to gradients can be rather low ($\sim 10^{13}$ W/cm^2) even for 1/4 μ light.

Fortunately collisional effects can reduce generation of these instabilities by short wavelength light. First, collisions introduce a threshold intensity which can be determined by balancing the growth rate with the collisional damping of the waves. At 1/4 n_{cr}, the collisional threshold for either instability is

$$I_T \sim \frac{4 \times 10^{10} Z^2}{\lambda_\mu^4 \theta_{keV}^3} \quad . \tag{14}$$

For a plasma with $Z = 3$ and $\theta_{keV} = 1$ irradiated with 1/4 μ light, $I_T \sim 10^{14}$ W/cm^2. Secondly, the incident light can be collisionally absorbed before it reaches a given density, an effect crudely estimated in Eq. 12. For a plasma with a local density scale length of $L = 2000$ μ and $Z = 3$, laser light with a wavelength of 1/4 μ is absorbed before 1/4 n_{cr} for $I < 5 \times 10^{14}$ W/cm^2.

There are a growing number of experiments[14-16] on Raman scattering in laser-irradiated plasmas as well as some rather detailed experiments[17] on the $2\omega_{pe}$ instability. In experiments with a large region of underdense plasma, Raman scattering as large as about 10% has been measured. In these experiments at LLNL,[16] a large region of underdense plasma was formed by irradiating a thin CH foil (7000Å thick) with a 1 ns, 2.5 kJ pulse of 1.06 μ light. This foil was predicted to expand through about 1/4 n_{cr} at about the peak of pulse, giving a large (∿ 400 μ) region of plasma for Raman scatter and the $2\omega_{pe}$ instability. Indeed, about 10% of the light was observed to the Raman scattered, most into the rear hemisphere, but even about one percent into the forward hemisphere. In addition, measurements with a streak camera showed that the forward-emitted 3/2 ω_0 light (a signature of plasma waves near 1/4 n_{cr}) and the high energy x-rays (a signature of heated electrons) were both correlated and came at the expected time in the laser pulse.

Brillouin Scattering

In addition to producing very energetic electrons which can preheat the target, there is also concern that plasma instabilities can significantly degrade the absorption. Here the principal culprit is the Brillouin instability, which represents the resonant decay of the incident light wave into a scattered light wave plus an ion acoustic wave. Since the ion sound frequency is much less than the light wave frequency, the Manley-Rowe relations show that nearly all of the energy of the incident photons can be transferred to scattered ones. Hence, if this instability were efficient, most of the laser light energy could be scattered away from the target. We note that the scattered light may still be absorbed before it leaves the plasma. This is particularly true for light side-scattered in a high-Z plasma.

Reflectivities of 50% or more have been computed for large, uniform regions of underdense plasma.[18] The threshold intensity is usually determined by gradients in the plasma. As representative, let's consider the threshold for Brillouin backscatter due to a gradient in the expansion velocity of the plasma:

$$I_T \sim \frac{7 \times 10^{15}}{L_\mu \lambda_\mu} \theta_{keV} \frac{n_{cr}}{n} \quad , \qquad (15)$$

where we have approximated the gradient length for expansion velocity by L_μ, the density scale length in microns. For a plasma with an electron temperature of 1 keV and a scale length near .1 n_{cr} of 2000 μ irradiated with 1/4 μ laser light, $I_T \sim 10^{14}$ W/cm^2.

A number of different experiments[18,19] indicate that sizeable Brillouin scatter is possible for high intensity light in large underdense plasmas. For example, in experiments at NRL[19] with 1.06 μ light at $I \sim 10^{16}$ W/cm^2, about 40% of the light was back reflected when a prepulse was used to prepare a sizeable region of underdense plasma. In these experiments, the frequency shift, intensity dependence of the reflectivity, and ray retrace properties of the reflected light confirmed that Brillouin scatter was responsible for the enhanced backscatter.

Filamentation

Lastly, the laser light can break up into intense filaments as it propagates through the underdense plasma. This enhancement in intensity can introduce other instabilities and aggravate deleterious collective effects. The filamentation can be driven by either ponderomotive[20] or thermal mechanisms.[21]

It's convenient to describe ponderomotive filamentation as convective growth with spatial gain coefficient κ_F. A threshold intensity I_T can then be estimated by the requirement $\kappa_{FIL}L > 1$, where L is the plasma size. If we use a quasi-static theory and neglect the ion pressure relative to the electron pressure,

$$I_T \sim \frac{3 \times 10^{15}\ \theta_{keV}}{L_\mu \lambda_\mu} \left(\frac{n_{cr}}{n}\right) \quad . \tag{16}$$

There is likewise a collisional threshold intensity determined by the condition $\kappa_{FIL}\lambda_{abs} > 1$, where λ_{abs} is the inverse bremsstrahlung absorption length. This threshold becomes

$$I_T \sim 3 \times 10^{12} \frac{Z}{\theta_{keV}^{1/2}} \frac{1}{\lambda_\mu^3} \left(\frac{n}{n_{cr}}\right) \quad . \tag{17}$$

If we use 1/4 μ light to irradiate a plasma with a density of .1 n_{cr}, an electron temperature of 1 keV, an ion charge state of 3, and a size of 2000 μ, $I_T \sim 10^{14} \frac{W}{cm^2}$.

In thermal filamentation, a local increase in intensity produces a density depression by the enhanced collisional heating and subsequent plasma expansion. Refraction of light into the density depression further increases the intensity, leading to instability. In the simplest model of thermal filamentation, we simply consider the propagation of a plane light wave through a slab of plasma. The plasma heating is described by balancing the inverse bremsstahlung absorption with the electron heat flow:

$$\nabla \cdot \kappa^T \nabla \theta_e = -\kappa I \quad , \tag{18}$$

where we are neglecting the contributions due to plasma flow. Here κ^T is the classical thermal conductivity, κ is the spatial damping coefficient for inverse bremsstrahlung, θ_e is the electron temperature, and I is the laser light intensity. To lowest order we assume no spatial variation in the intensity of the light except in the direction of propagation (x-direction). We then have

$$\frac{d}{dx} \kappa_o^T(x) \frac{d\theta_{eo}}{dx} = -\kappa_o I_o(x) \quad , \tag{19}$$

where the subscript o denotes lowest order. For a given density $n_o(x)$, this equation determines the temperature $\theta_{eo}(x)$ consistent with the heating.

We next introduce a small perturbation in the light intensity transverse to the direction of propagation; i.e. $I = I_o(x) [1 + \alpha \cos ky]$. This intensity perturbation will create a perturbation in temperature, which in turn leads to a variation in density. In the quasi-static limit, the density perturbation is readily calculated from the energy balance equation, giving

$$n = n_o(x) \left[1 - \frac{\kappa_o I}{k^2 \kappa_o^T \theta_{eo}} \right] . \tag{20}$$

The growth of filamentation is finally obtained by solving the wave equation with this intensity-dependent density. The maximum spatial gain coefficient becomes

$$\kappa_g^{th} \simeq \frac{1}{7} \frac{\omega_{pe}}{\omega_o} \frac{v_{os}}{v_e} \frac{1}{\lambda_{mfp}} \quad , \tag{21}$$

where we have assumed that $k\lambda_{mfp} >> 1$ and $Z >> 1$. Here v_{os} is the electron oscillatory velocity in the light wave, v_e is the electron thermal velocity, and λ_{mfp} is an electron mean-free-path (v_e/ν_{ei}, where ν_{ei} is given in Eq. 2).

Thermal filamentation can be quite significant in dense, cold plasmas produced by irradiation with short wavelength laser light. It has a greater spatial gain than does ponderomotive filamentation provided $\frac{\nu_{ei}}{\omega_{pe}} > \frac{v_{os}}{c}$, where ν_{ei} is the electron-ion collision frequency. We will estimate a threshold intensity, I_T, by the condition that growth occurs before the light is collisionally absorbed; i.e., by $\kappa_g^{th} \ell_{abs} \sim 1$:

$$I_T \simeq 1.6 \times 10^{14} \frac{n}{n_{cr}} \frac{\theta_{keV}^2}{\lambda_\mu^2} \quad . \tag{22}$$

If we use 1/4 μ light to irradiate a plasma with a density of .1 n_{cr} and an electron temperature of 1 keV, $I_T \sim 2 \times 10^{14}$ W/cm^2. Note that this threshold intensity had very little dependence on wavelength, since the electron temperature is expected to decrease as the wavelength decreases.

There have been many indications that filamentation is playing some role in laser-plasma experiments.[21,22] However, the evidence is generally indirect and difficult to quantify. Very little is known about the nonlinear consequences of filamentation, either ponderomotive or thermal. This remains a potentially very important area for ongoing research.

Summary

In summary, we have given a brief overview of important laser-plasma coupling processes and have estimated the intensity-wavelength regime in which the various processes can be significant. If we use short wavelength laser light, collisional absorption is quite potent over a substantial range of intensities. Recent experiments with short wavelength light and small underdense plasmas indeed show a significant regime of high absorption.

Minimizing collective effects in reactor-size plasmas can impose more substantial restraints on the intensity. There is growing experimental evidence[23] that instabilities can become more potent as the size of the underdense plasma increases; i.e., as instability thresholds due to plasma inhomogeneity decrease. However, there still appears to be a promising regime for target design in which collisional absorption is high and collective effects are minimized. The crude estimates presented here indicate that this regime is accessible with short wavelength ($\sim$ 1/2 - 1/4 μ) laser light at an intensity of order 10^{14} W/cm^2. Clearly more calculations and experiments are needed with larger regions of underdense plasma to more quantitatively define this very promising intensity-wavelength window for laser fusion applications.

Acknowledgments

The manuscript is based on an invited lecture presented at the 1983 Spring College on Radiation in Plasmas (Trieste, Italy) and represents an extension of the papers in Reference 3. I am grateful for discussions with M. Campbell, P. Drake, K. Estabrook, M. Herbst, B. Langdon, B. Lasinski, C. Max, W. Mead, D. Phillion and R. Turner.

Table I: A partial list of the instabilities which can be driven by laser light propagating in plasma. Here ω_{pe} is the electron plasma frequency, ω_{ia} is the ion accoustic frequency, and ω_o (ω_{sc}) is the frequency of the incident (scattered) light wave.

Resonant coupling of laser light into two other waves

- Ion acoustic decay instability $\omega_0 \rightarrow \omega_{pe} + \omega_{ia}$ at $n \simeq n_{cr}$
- Two plasmon decay instability $\omega_0 \rightarrow \omega_{pe} + \omega_{pe}$ at $n \simeq 1/4\, n_{cr}$
- Raman instability $\omega_0 \rightarrow \omega_{sc} + \omega_{pe}$ at $n \lesssim 1/4\, n_{cr}$
- Brillouin instability $\omega_0 \rightarrow \omega_{sc} + \omega_{ia}$ at $n \lesssim n_{cr}$

Filamentation Light 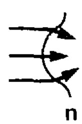

at $n \lesssim n_{cr}$

TABLE I

REFERENCES

1. R. E. Kidder, in Physics of High Energy Density, edited by P. Caldirola (Academic, New York, 1971), p. 306; J. H. Nuckolls, L. Wood, A. Thiessen and G. Zimmerman, Nature 239, 139 (1972).
2. C. E. Max and K. G. Estabrook, Comm. Plasma Phys. Cont. Fusion 5, 239 (1980); C. E. Max in Laser-Plasma Interaction, edited by R. Balian and J. C. Adam (North Holland, Amsterdam, 1982).
3. W. L. Kruer, Comm. Plasma Phys. Cont. Fusion 6, 167 (1981); W. L. Kruer, in Laser Plasma Interactions 2, edited by R. A. Cairns (SUSSP Publications, Edinburg, 1983).
4. N. G. Basov, et al., Sov. J. Quantum Electron, 2, 439 (1973); C. Garban-Labaune et al., Phys. Rev. Lett. 48, 1018 (1981); W. Seka et al., Opt. Commun. 40, 437 (1982).
5. D. C. Slater et al., Phys. Rev. Lett. 46, 199 (1981); H. Nishimura et al., Phys. Rev. A 23, 2011 (1981); F. Amiranoff et al., Phys. Rev. Lett. 43, 522 (1979).
6. W. C. Mead et al., Phys. Rev. Lett. 47, 1289 (1981).
7. T. W. Johnston and J. M. Dawson, Phys. Fluid 16, 722 (1973).
8. A. B. Langdon, Phys. Rev. Lett. 44, 575 (1980).
9. A. R. Bell, R. G. Evans and D. J. Nicholas, Phys. Rev. Lett. 46, 243 (1981); and references therein.
10. K. G. Estabrook, E. J. Valeo and W. L. Kruer, Phys. Fluids 18, 1151 (1975); D. W. Forslund, J. M. Kindel, K. Lee E. Lindman, and R. L. Morse, Phys. Rev. A11, 679 (1975); A. B. Langdon, Phys. Rev. Lett. 22, 1794 (1980).

11. J. J. Thomson and W. L. Kruer, Comm. Plasma Phys. Cont. Fusion 4, 13 (1978) and references therein.

12. P. K. Kaw, W. L. Kruer, C. S. Liu and K. Niskikawa, Advances in Plasma Physics (Wiley, New York, 1976), Vol. 16, p. 1-270.

13. A. B. Langdon, B. F. Lasinski, and W. L. Kruer, Phys. Rev. Lett. 43, 113 (1979); and references therein.

14. J. L. Bobin, M. Decroisette, B. Meyer and Y. Vittel, Phys. Rev. Lett. 30, 594 (1973); R. G. Watt, R. D. Brooks and Z. A. Pietrzyk, Phys. Rev. Lett. 41, 170 (1978); C. Joshi, et al., Phys. Rev. Lett. 47, 1285 (181); K. Tanaka et al., Phys. Rev. Lett. 48, 1179 (1982); J. Elazar, W. Toner and E. R. Wooding, Plasma Phys. 23, 813 (1981).

15. A. A. Offenberger, R. Fedosejevs, W. Tighe, and W. Rozmus, Phys. Rev. Lett. 49, 371 (1982).

16. D. W. Phillion et al., Phys. Rev. Lett. 49, 1405 (1982); D. W. Phillion et al., Phys. Fluids 25, 1434 (1982).

17. N. A. Ebrahim, H. A. Baldis, C. Joshi and R. Benesch, Phys. Rev. Lett. 45, 1179 (1980); and references therein.

18. W. L. Kruer, Comm. Plasma Phys. Cont. Fusion 4, 13 (1978).

19. B. H. Ripin et al., Phys. Rev. Lett. 39, 611 (1977).

20. B. I. Cohen and C. E. Max, Phys. Fluids 22, 1115 (1979).

21. M. J. Herbst, J. A. Stamper, R. H. Lemberg, R. R. Whitlock, F. C. Young, J. Grun and B. H. Ripin, in Proceedings of the 1981 Topical Conference on Symmetry Aspects of Inertial Fusion Implosions, Edited by S. Bodner; M. J. Herbst et al., Phys. Rev. Lett. 32, 1234 (1974); D. Subbaro and M. S. Sodha, J. Appl. Phys. 50, 4604 (1979) and references therein.

22. C. E. Max et al., Lawrence Livermore National Laboratory, UCRL-88056 (1983).

23. E. M. Campbell et al., Lawrence Livermore National Laboratory UCRL-88055 (1983).